Structure of Zinc-Substituted Cytochrome *c*: Nuclear Magnetic Resonance and Optical Spectroscopic Studies†

Helen Anni,* Jane M. Vanderkooi, and Leland Mayne

Department of Biochemistry and Biophysics, School of Medicine, University of Pennsylvania, Philadelphia, Pennsylvania 19104

Received October 17, 1994; Revised Manuscript Received January 16, 1995⊗

ABSTRACT: Optical and proton nuclear magnetic resonance (NMR) studies were carried out to assess the structure of the polypeptide chain and metal ligation in zinc-substituted horse heart cytochrome *c* (Zn Cyt *c*). The 1D- and 2D-NMR (COSY, TOCSY, and NOESY) spectra allowed the assignment of proton resonances in 67 amino acid residues. These residues arose from all structural elements of the protein, α-helices, β-turns, and segments of the protein with no defined secondary structure. Small deviations of the chemical shifts of Zn Cyt *c* proton resonances from native Fe(II) Cyt *c* of less than 0.1 ppm are due to not fully matching solvent conditions. Differences in the chemical shifts between the two proteins in the range 0.10−0.20 ppm are not clustered and are observed not only in the vicinity of the Zn porphyrin but also on distant surface locations of the cytochrome. The resonance positions of the bridge protons, from the thioether bonds of the porphyrin with Cys 14 and Cys 17, were conserved in Zn Cyt *c*. Similarly, the Met 80 and His 18 protons had chemical shifts supporting the proposal that His 18 and Met 80, as for Fe(II) Cyt *c*, may provide the axial ligation in the Zn protein and that zinc may be in an unusual hexacoordinated geometry. Chemical shifts from proton resonances of alternative axial ligands of misfolded cytochrome like His 33, Lys 79, and Phe 82 were found to be the same as in the Fe(II) protein, excluding the possibility of their axial ligation to Zn. The His 18-Zn-Met 80 ligation was also consistent with data from absorption and luminescence studies. We conclude that Zn Cyt *c* is an adequate structural model for Fe(II) Cyt *c* as both share the same overall structure, including axial ligands, environment in the porphyrin vicinity, and the same binding interface with redox partners.

Metal-substituted porphyrin proteins serve as models of the native iron proteins in several capacities, and in particular, metal derivatives of cytochrome *c* (Cyt *c*)[1] have been extensively used in luminescence studies. Areas of research have included examination of distance determinations with redox partners (Vanderkooi et al., 1977, 1980; Koloczek et al., 1987), excited-state electron-transfer reactions (Ho et al., 1985; Liang et al., 1986; Zhou & Hoffman, 1994), and the effect of the polypeptide chain on the electronic structure of the porphyrin (Logovinsky et al., 1993). In spite of this widespread interest in Cyt *c*, it is not certain how changing the central metal with one of different size and possibly different ligation modalities impacts the overall folding and stability of the protein. It is known that, in the absence of heme, apo-Cyt *c* is largely disordered (Stellwagen et al., 1972; Fisher et al., 1973; Hamada et al., 1993) and that iron ligation comes later in the folding sequence of globular proteins to stabilize the structure (Babul & Stellwagen, 1972). The iron is ligated to the protein even in denatured Cyt *c*, after much of the secondary structure is gone (Babul & Stellwagen, 1971; Muthukrishnan & Nall, 1991).

The purpose of this work is to examine in what way replacement of Fe with Zn in Cyt *c* may affect the protein structure. In terms of size and charge Zn(II) resembles Fe(II). Under some disease conditions where iron metabolism is impaired, Zn substitutes for Fe(II) in a small fraction of the heme proteins (Vanderkooi & Landesberg, 1977). Since a living cell is intolerant of wrongly folded proteins, this experiment of nature suggests that the structure of Zn-substituted heme proteins is very close to the normal iron derivatives. Unlike d^6 Fe(II), Zn(II) is a d^{10} metal and consequently has no empty d orbital for redox reactions. Zn porphyrins are closed-shell metalloporphyrins that have two additional antibonding σ^* electrons in d_{z^2} and $d_{x^2-y^2}$ orbitals, not present in low-spin Fe(II) porphyrins (Gouterman, 1959). The strong influence of the antibonding electrons of Zn are offset by its much stronger Lewis acid properties (large electrostatic contribution) in comparison to Fe(II) (Vogel & Stahlbush, 1977; Nappa & Valentine, 1978).

In this paper, the fold of the polypeptide chain in Zn(II) Cyt *c* and the ligation of Zn are examined by proton 1D- and 2D-nuclear magnetic resonance (NMR) techniques and compared with Fe(II) Cyt *c*. Because the immediate environment of the porphyrin is of prime importance in determining "reactivity", the properties of the porphyrin are additionally inspected by optical absorption, fluorescence, and phosphorescence spectroscopy for evidence of ligation.

MATERIALS AND METHODS

Materials. Sodium or potassium phosphate and tris(hydroxymethyl)aminomethane (TRIS) buffers were made

† Supported by grants from the NIH [P01-GM48130 (J.M.V., H.A.) and DK11295 (L.M.)], the International Human Frontier of Science Program [RE-331/93 (L.M.)], and the University of Pennsylvania Research Foundation (H.A.).

* Corresponding author [telephone (215) 898-0573 and 898-8783; FAX (215) 573-2042; email ANNI@A1.MSCF.UPENN.EDU].

⊗ Abstract published in *Advance ACS Abstracts,* March 1, 1995.

[1] Abbreviations: Cyt *c*, cytochrome *c*; Zn Cyt *c*, zinc(II)-substituted cytochrome *c*; MP, mesoporphyrin IX; Zn(MP), zinc mesoporphyrin IX; Zn(MP-DME), zinc mesoporphyrin dimethyl ester; Mb, myoglobin; Zn(MP)-Mb, zinc mesoporphyrin myoglobin; NMR, nuclear magnetic resonance; COSY, *J*-correlated spectroscopy; NOESY, nuclear Overhauser effect spectroscopy; TOCSY, total correlation spectroscopy; FID, free induction decay.

0006-2960/95/0434-5744$09.00/0

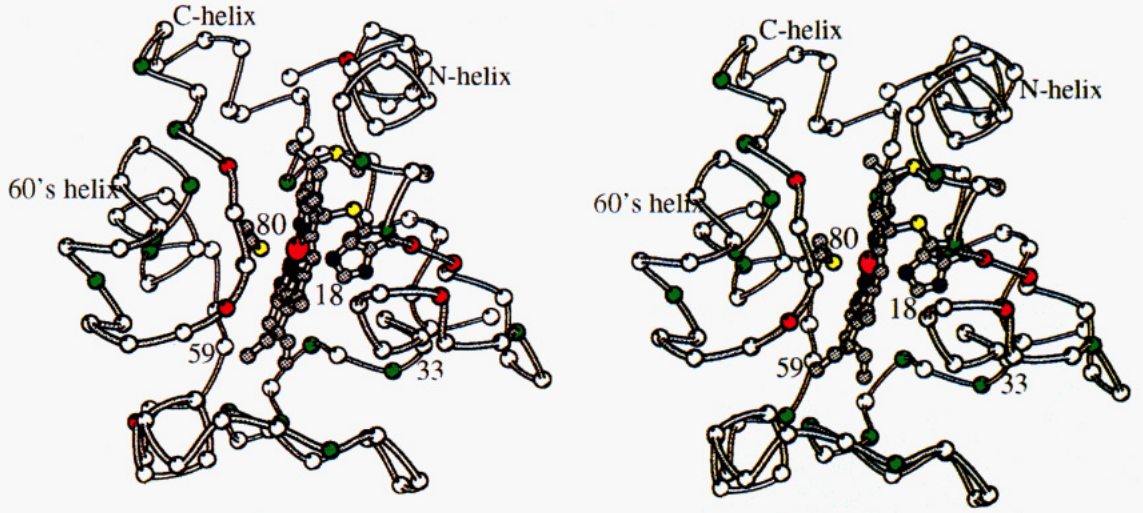

FIGURE 1: Diagram of the structure of horse Fe(II) Cyt *c* drawn with the program MOLSCRIPT (Kraulis, 1991). Data are taken from the 1.94 Å resolution crystal structure (Bushnell et al., 1990). The locations of the α carbons are shown for all residues. Also shown are ball-and-stick representations of the heme, the side chains of its axial ligands His 18 and Met 80, and its covalent attachments at Cys 14 and Cys17 (sulfur atoms are in yellow). The chemical shift differences for the backbone proton resonances between Zn and Fe(II) Cyt *c* are indicated by color: protons that have shifts of less than 0.1 ppm are shown in white; green is used for protons that have shifts in the range of 0.1−0.2 ppm and red for those with shifts greater than 0.2 ppm.

with analytical grade reagents. Glass-distilled water was used throughout. Zinc mesoporphyrin IX [Zn(MP)] and its dimethyl ester [Zn(MP-DME)] were obtained from Porphyrin Products (Logan, UT). Zn porphyrins were dissolved in "neat" toluene or pyridine that provide respectively a noncoordinating or a coordinating solvent. Glycerol, horse heart Cyt *c* type III, and horse myoglobin (Mb) were obtained from Sigma Chemical Co. (St. Louis, MO).

Zn(II) Cyt *c* was prepared from horse heart Cyt *c* as previously described (Vanderkooi & Erecinska, 1975; Vanderkooi et al., 1976). The Zn(MP)-Mb preparation from horse myoglobin was done according to Papp et al. (1990).

Spectroscopy. Absorption spectra were obtained with a Hitachi U-3000 spectrophotometer. Fluorescence, delayed fluorescence, and phosphorescence spectra were acquired with a Perkin-Elmer LS-5 fluorometer. Phosphorescence lifetimes were determined using instrumentation described earlier (Green et al., 1988). Phosphorescence spectra and lifetimes were measured at 77 K in 50% glycerol (v/v).

Proton NMR spectra were collected at 20 and 35 °C on a Bruker AM-500 (500 MHz) NMR spectrometer. Zn Cyt *c* (3 mM) was in 50 mM phosphate buffer, pH 6, containing 10% D_2O for frequency lock. Chemical shifts (in ppm) were referenced to TSP [sodium 3-(trimethylsilyl)tetradeuteriopropionate] added as an internal standard. *J*-correlated spectra (COSY) were collected in the magnitude mode (Nagayama et al., 1980) with 512 t_1 free induction decays (FIDs) of 1024 complex data points. Each FID was the sum of 96 transients. The spectral width was 9090.9 Hz in both dimensions. The solvent signal was suppressed by presaturation. Nuclear Overhauser effect spectra (NOESY) (Macura & Ernst, 1980) and total correlation spectra (TOCSY) (Bax & Davis, 1985) were acquired as above with time-proportional phase incrementation (TPPI) in t_1 (Redfield & Kuntz, 1975; Marion & Wüthrich, 1983). The NOESY spectra had a mixing time of 80 ms. The TOCSY mixing time was 39.6 ms using MLEV 16. The 2D-NMR data were processed on a Silicon Graphics computer using the program Felix (Hare Research).

Graphics. The coordinates for horse heart Cyt *c* were obtained from Bushnell et al. (1990). Graphics were done with the program Insight II (Biosym Inc.) on a Silicon Graphics workstation. Distances were measured from the crystal structures deposited in the Brookhaven Protein Data Bank. For yeast iso-1 Fe(II) Cyt *c* we used the entry 1YCC (Louie & Brayer, 1990), for the corresponding Fe(III) Cyt *c* the entry 2YCC of the Cys 102 → Thr 102 variant (Berghuis & Brayer, 1992), and for deoxy sperm whale Mb the entry 5MBN (Takano, 1977).

RESULTS

NMR Spectroscopy. The NMR spectroscopy data are discussed in reference to the structure of horse Fe(II) Cyt *c*, shown as an α-carbon trace in Figure 1. The chemical shifts of proton resonances of Zn Cyt *c*, along with their differences from the literature values of Fe(II) Cyt *c* (Wand et al., 1989; Feng et al., 1990a,b) are compiled in Table 1. Chemical shifts differences for backbone and side-chain proton resonances are also given in histogram form in Figure 2. The Zn Cyt *c* proton resonances were obtained from spectra such as shown in Figure 3, where the fingerprint region of the magnitude COSY-NMR spectrum of Zn Cyt *c* is presented. The assignments were verified by TOCSY (Figure 4), NOESY (not shown), and/or 1D-NMR spectra (Figure 5).

The overall folding and both α-helices and β-turns appear to be conserved in Zn Cyt *c*, because the chemical shifts of the majority of backbone NH and CαH resonances are the same as in Fe(II) Cyt *c* (Table 1). This is clearly indicated in Figure 1, where backbone protons that have shifts of less than 0.1 ppm are in white balls. As a result of small deviations of experimental conditions most backbone protons have chemical shift differences from Fe(II) Cyt *c* of 0.05 ppm (Figure 2).

There are 20 residues (in green) in Figure 1 with chemical shifts of backbone resonances differing by 0.1−0.2 ppm between the Fe(II)- and Zn-containing proteins. These residues are scattered throughout the protein. On the right side of Figure 1, **Gly 24** is in the middle of a surface β-loop,

Table 1: Chemical Shifts (in ppm) of Assigned Proton Resonances of Zn Cyt *c* at 20 °C and Differences from Fe(II) Cyt *c*[a]

residue	NH	CαH	CβH	CγH	CδH	other
Asp 2	9.22	4.71	2.77, 2.51			
	0.21	0.09	0.05, 0.00			
Val 3	8.55	3.61	2.13			1.08 $C\gamma H_3$
	0.06	0.05	0.06			0.01
Glu 4	8.17	4.09	2.13, 2.17	2.36		
	0.00	0.03	−0.02, 0.01	0.00		
Gly 6	8.80	4.21, 3.57				
	0.09	−0.01, 0.01				
Lys 7	8.10	2.27	1.79	1.60, 1.39	1.03	
	0.04	0.06	−0.01	0.02, 0.03	*−0.13*	
Lys 8	6.97	3.91	1.88	1.39	1.71	3.09 $C\epsilon H$
	0.04	0.03	0.08	0.04	−0.01	−0.10
Phe 10	8.67	4.03	3.09, 3.04			6.18 C_5H, 7.20 C_6H
	0.05	0.03	0.03, −0.04			−0.06, −0.02
Val 11	8.80	3.50	2.11			1.08, 0.92 $C\gamma H_3$
	0.02	0.08	0.08			0.06, 0.05
Lys 13	8.97	5.05	2.45		1.97	3.16 $C\epsilon H$
	0.04	0.00	0.07		0.08	0.04
Cys 14	8.39	5.49	1.15, 1.76			bridge 2: 5.44 CH, 1.51 CH_3
	0.00	*−0.14*	−0.01, *0.12*			**−0.21**, −0.02
Ala 15	7.41	4.03				
	0.03	−0.09				
Gln 16	8.88	3.94	2.24, 2.01	2.79, 2.54		
	−0.01	0.05	0.05, 0.05	−0.05, −0.02		
Cys 17	6.95	4.09	0.71			bridge 4: 6.42 CH, 2.63 CH_3
	0.08	*0.14*	−0.10			−0.06, −0.02
His 18	6.20	3.77	0.82, 0.85			0.59 C_2H, 9.51 $N\pi H$
	0.21	*−0.12*	−0.03, **0.23**			*−0.18*, 0.10
Thr 19	7.94	4.21	4.46			1.17 $C\gamma H_3$
	−0.08	**0.32**	0.00			−0.07
Lys 22	8.83	3.16	0.48			
	0.07	−0.01	0.10			
Gly 23	9.15	3.54, 3.86				
	0.09	0.01, 0.00				
Gly 24	7.69	3.13, 3.80				
	0.12	0.00, 0.02				
Lys 27	7.53	4.42	1.03			
	0.26	0.05	*0.11*			
Leu 32						−0.87, −0.65 $C\delta H_3$
						0.11, 0.04
His 33	7.48	3.86	2.97, 3.00			
	0.08	−0.06	−0.02			
Gly 34	8.81	3.87, 3.73				
	0.12	0.06, 0.01				
Phe 36	8.60	3.94	3.22, 2.83			6.84 C_3H/C_5H, 7.11 C_4H
	0.11	0.05	0.02, 0.04			0.04, 0.01
Gly 37	9.43	4.46				
	0.10	0.02				
Arg 38	8.55	4.78	2.17, 2.11			
	−0.18	−0.04	0.00, −0.02			
Lys 39	8.12	4.96	1.56			
	0.03	0.03	0.05			
Thr 40	7.23	4.32	4.42			0.87 $C\gamma H_3$
	0.16	*0.18*	0.04			0.02
Gly 45	9.12	4.39, 3.78				
	0.06	−0.02, 0.05				
Phe 46	7.13	4.18	1.12			
	0.06	−0.01	0.00			
Thr 47	7.28	4.14				
	0.04	*0.15*				
Tyr 48	8.51	5.22	2.81			7.68 C_2H, 7.11 C_3H, 8.55 $O\beta H$, 7.25 C_5H
	0.02	0.01	0.00			**0.31**, −0.02, *0.14*, 0.04
Asp 50	8.83	4.37	2.56			
	0.02	0.02	0.05			
Lys 53	8.10	3.59	1.85	1.37		
	0.00	−0.01	0.03	*0.19*		
Asn 54	8.76	4.55	2.93, 2.97			
	−0.01	−0.01	*−0.16*, *−0.18*			
Lys 55	7.50	3.85				
	−0.01	**0.21**				
Ile 57	6.36	4.35	1.79	0.82		0.69 $C\gamma H_3$, −0.59 $C\delta H_3$
	0.03	0.05	0.04	0.07		0.04, 0.06
Thr 58	8.12	4.09	3.84			
	0.05	*0.16*	−0.07			
Trp 59	8.94	4.87	2.49			6.98 C_2H, 10.02 NH, 7.53, 6.61, 5.63, 7.07 C_4H-C_7H
	0.08	0.01	0.02			0.01, 0.01, 0.05, 0.07, 0.10, −0.02
Glu 62	9.51	4.05	2.01	2.40		
	0.18	0.05	0.10	0.03		

Table 1 (Continued)

residue	NH	CαH	CβH	CγH	CδH	other
Thr 63	7.14	4.26				
	0.09	0.09				
Leu 64	8.81	4.35				
	0.08	0.00				
Met 65	8.49	3.94	2.24, 2.01	2.68, 2.63		
	0.08	0.05	*0.13*, 0.08	0.08, 0.01		
Glu 66	6.66	4.05				
	0.09	0.01				
Tyr 67	8.26	3.73				
	0.01	*−0.11*				
Leu 68	8.23	3.09				0.37, 1.15 CδH$_3$
	0.11	0.03				−0.01, −0.08
Glu 69	6.88	3.89	1.51	2.03, 1.97		
	0.03	0.06	**0.25**	*0.17*, *0.14*		
Asn 70	6.20	4.21	3.07, 3.04			
	0.04	0.06	**−0.25**, **−0.24**			
Lys 73	6.97	3.91	1.88			
	0.04	0.06	−0.22			
Tyr 74	7.27	4.26				
	0.05	*0.11*				
Gly 77	8.62	4.19, 3.61				
	0.09	0.02, 0.01				
Thr 78	8.17	4.54		1.01		8.42 OβH
	−0.01	−0.02		*−0.20*		−0.02
Lys 79	7.76	4.51	1.97, 2.36			
	0.21	*0.12*	−0.01, −0.04			
Met 80	7.13	3.13	−0.12, −2.58	−3.68, −1.58		−3.07 CεCH$_3$
	0.01	−0.03	−0.09, −0.01	−0.07, **−0.30**		**−0.21**
Ile 81	7.98	3.55	2.01			
	−0.01	0.03	0.06			
Phe 82	6.41	4.09	0.71, 2.15			6.59 C$_2$H/C$_6$H, 7.55 C$_3$H/C$_5$H
	0.18	**0.21**	−0.10, 0.03			*0.11*, −0.06
Ala 83	8.26	3.73	1.07			
	0.01	*−0.11*	0.03			
Lys 86	8.55	4.02	1.85			
	0.14	0.05	−0.01			
Lys 88	9.01	3.66				
	0.07	0.05				
Glu 90	6.31	4.26	1.99, 2.03	2.36		
	0.05	0.02	0.02, 0.05	0.01		
Glu 92	8.53	3.94	2.24	2.54		
	0.08	−0.03	0.07	0.04		
Ile 95	8.90	3.70	2.03			1.24 CγH$_3$
	0.13	0.03	0.08			−0.04
Leu 98	9.04	3.39	2.31	2.26		1.08, 0.60 CδH$_3$
	0.10	0.07	0.01	−0.06		0.03, 0.09
Lys 99	8.97	2.59	1.53, 1.31	0.73, 0.52	3.54	2.43 CεH, 7.27 NεH
	0.10	*0.12*	0.06, 0.01	0.04, −0.08	**−0.26**	*0.13*, *−0.20*
Lys 100	6.77	4.03	1.69, 1.85	1.42, 1.62		
	0.09	0.06	0.08, −0.08	*−0.17*, 0.06		
Ala 101	8.58	3.84	0.50			
	0.10	0.06	0.07			
Asn 103	7.00	4.87	2.77, 2.49			
	0.08	0.00	0.07, 0.05			
Glu 104	7.18	4.19	1.99			
	0.07	0.03	0.03			

[a] Experimental conditions are given in Materials and Methods. Chemical shift differences (Fe−Zn) of more than 0.20 ppm are shown in boldface type. Those in the range 0.10−0.20 ppm are in italic type. All differences are presented in the second row. Amino acids in boldface indicate invariant residues in cytochrome *c*.

Gly 34 and **Phe 36** participate in two short β-turns, and **Thr 40** and **Thr 47** are in a part of the protein without a defined secondary motif that wraps the heme edge. On the left side of Figure 1, **Thr 58** is in a coiled region, as well as **Lys 79**, **Phe 82**, **Ala 83**, and **Lys 86**, whereas **Glu 62**, **Tyr 67**, **Leu 68**, and **Tyr 74** are in α-helical protein segments. The Tyr 67 OH group hydrogen-bonds to the Met 80 SD in Fe(III) Cyt *c* (Bushnell et al., 1990). Finally, **Ile 95** and **Lys 99** are located in the N-terminal largest α-helix in the protein. All assigned proton resonances of **Arg 38** in Zn Cyt *c* are identical to those of the Fe(II) protein except the backbone NH. Nevertheless, it is the side-chain NH of Arg 38 that has been suggested from the crystal structure to be hydrogen-bonded to propionate 1 of porphyrin's pyrrole A (Bushnell et al., 1990). Around the porphyrin, the CαH of **Cys 14**, **Cys 17**, and **His 18** are also somewhat changed in Zn Cyt *c*. In Figure 1, the heme, the side chains of its axial ligands His 18 and Met 80, and its covalent attachments at Cys 14 and Cys17 are shown in ball-and-stick representations with sulfur atoms in yellow.

Backbone proton resonances with chemical shifts different from Fe(II) Cyt *c* by more than 0.2 ppm are colored red in Figure 1. Noticeably, there are seven such residues: **Asp 2** in the C-terminal coil, **Lys 27** on the same side as His18 in a coiled conformation segment that serves to cover the front of the heme, and **Lys 55** also in a coiled part of the protein. These residues are located away from the Zn porphyrin. Differences are also observed around the axial ligands and

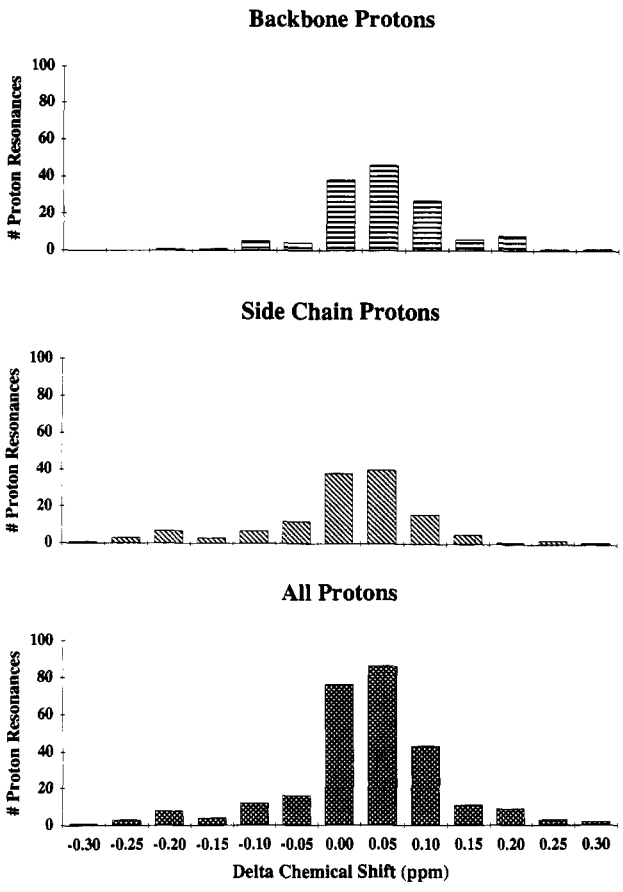

FIGURE 2: Histogram showing the distribution of chemical shift changes between Zn and Fe(II) Cyt *c* for all the measured proton resonances: from backbone (top), side chains (middle), and cumulative (bottom).

neighboring residues **His 18** (NH), **Thr 19** (CαH), **Lys 79** (NH), and **Phe 82** (CαH). Although these chemical shift differences between the Fe(II) and Zn protein are considered significant, they are smaller (by more than an order of magnitude) in comparison to the corresponding differences between these proteins and a random coil (data not shown) (Wüthrich, 1986). These data are consistent with the lack of any secondary structure disruption in the Zn-substituted protein.

Other residues in the vicinity of **Lys 55** are unaffected by the metal substitution in the porphyrin with Zn (Figure 1). A striking example is **Ile 57** that has been completely assigned and has even side-chain protons in place (Table 1, Figure 5). The last residue, **Trp 59**, of this protein coil formed by residues 55−59 has been used as a marker for folding via energy transfer (Vanderkooi et al., 1976). The side-chain ring NH of Trp 59 is hydrogen-bonded to propionate 2 of porphyrin pyrrole A (Bushnell et al., 1990). Proton resonances from both Trp 59 rings could be detected, and their chemical shifts were less than 0.1 ppm different from those observed in Fe(II) Cyt *c*. These results indicate that the Trp 59 hydrogen bond to the porphyrin most probably is intact.

The axial ligand to Fe Cyt *c*, **His 18**, is in a coil conformation structural element defined by residues 18−20. The chemical shifts for the backbone NH and CαH resonances of His 18 in Zn Cyt *c* are displaced relative to Fe(II) Cyt *c* by 0.21 and 0.12 ppm, respectively. The largest difference in the proton resonances between the two proteins, 0.32 ppm, was found for the chemical shift of the following residue, **Thr 19** CαH, but the chemical shifts for the other protons in this residue are the same as in Fe(II) Cyt *c*. Of particular note is that the resolved proton resonances of His 33, an alternative axial ligand of misfolded Fe Cyt *c* (Babul & Stellwagen, 1971; Muthukrishnan & Nall, 1991), are not affected by the change of metal.

Also noteworthy are the chemical shifts of the invariant **Lys 79** and **Phe 82** residues (Table 1, Figure 1). Phe 82 participates in the conformation of remote protein sites (Louie et al., 1988; Louie & Brayer, 1989), and it can push Met 80 away from the metal coordination site to become the axial ligand (Hawkins et al., 1994). This residue modulates also the electron-transfer reaction rates with Cyt *c* peroxidase (Liang et al., 1987). Moreover, the packing of Phe 82 and Ile 81 in solution is different from that in the crystal (Qi et al., 1994). One backbone proton had an altered chemical shift in both Lys 79 and Phe 82, by 0.21 ppm in comparison to Fe(II) Cyt *c*, indicating that the position of this residue did somewhat change with metal substitution. Nevertheless, axial ligation of either Lys 79 or Phe 82 is excluded, because of the relatively small chemical shift difference and the finding that the chemical shifts of **Met 80** backbone resonances, that serves as the second axial ligand in Fe(II) Cyt *c*, are strikingly the same in Zn Cyt *c* (Table 1, Figure 1).

Although Met 80 is in a coil fragment of the protein formed by residues 79−86, its chemical shifts for backbone resonances are considerably upshifted relative to Met in random coil (NH, 8.42 ppm; CαH, 4.52 ppm) (Wüthrich, 1986). Moreover, in the 1*D*-NMR spectrum (Figure 5) the resonances of Met 80 side-chain protons are located in the upfield region (from 0 to −4.0 ppm). These resonances are shifted by strong ring current effects due to their proximity to the heme. The resonances for CβH (two protons), CγH (two protons), and CεCH$_3$ are well resolved and close to the case for the Fe(II) protein. The largest difference is observed for one of the CγH resonances; it shows a chemical shift to −1.58 ppm in Zn Cyt *c* instead of −1.88 ppm. Since these protons are on either side of the liganding sulfur (SD), at a distance of less than 2 Å (Figure 1), the Met 80 sulfur in the two proteins should remain in nearly the same position. The ring current shifts are strongly dependent on the distance from the aromatic group to the shifted proton. The magnitude of the changes in chemical shift seen between the Zn and Fe(II) Cyt *c* indicates that any geometry changes must be less than 1 Å (Wüthrich, 1986). Taken together, the backbone and side-chain proton resonances of Met 80 demonstrate the existence of a thioether bond between Met 80 and Zn. We note, however, that there are shifts in the resonances of the Met 80 side-chain protons with temperature (Figure 5), in agreement with Moore et al. (1980). Furthermore, the intensity of the resonance at −3.07 ppm decreased at higher temperatures. Unlike Zn Cyt *c*, in this temperature range (20−40 °C) the same proton resonances of Met 80 for Fe(II) Cyt *c* do not vary (Wand et al., 1989; Feng et al., 1990a). These data point to a reduced stability of the Zn protein, at least as it concerns the porphyrin and Met 80 environment.

There are no significant differences in the chemical shifts of side-chain resonances between Zn and Fe(II) Cyt *c* with the following exceptions: **His 18** (CβH), **Tyr 48** (C$_2$H), **Glu 69** (CβH), **Asn 70** (CβH), **Lys 73** (CβH), and **Lys 99** (CδH) (Table 1, Figure 2). The two proteins are in general

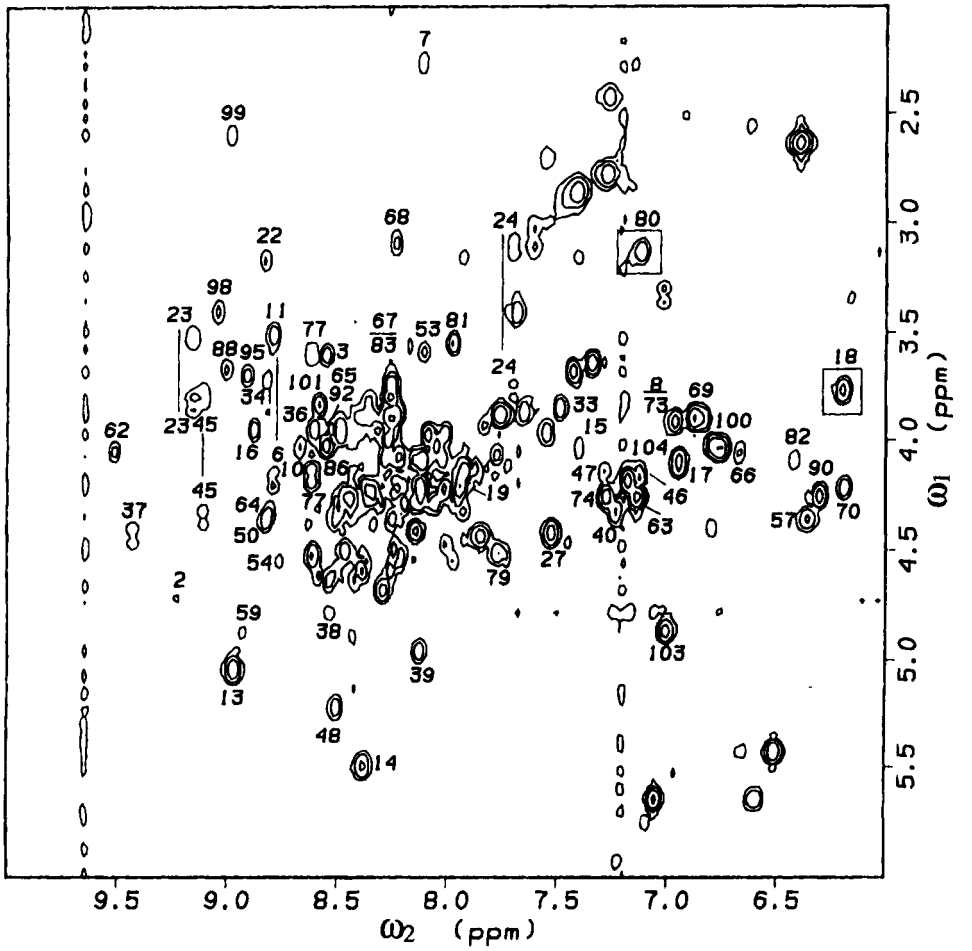

FIGURE 3: Fingerprint region of the magnitude COSY-NMR spectrum of Zn Cyt *c* at 20 °C.

remarkably similar, and as expected, the distribution of the chemical shift differences is wider for the side-chain protons in comparison to backbone protons (Figure 2). Additionally, the β-turn residue 14−17 fragment that includes Cys 14 and Cys 17, the residues that covalently condense with the vinyl groups of the porphyrin at positions 2 and 4, shows no significant changes in chemical shifts for all four residues (Table 1, Figure 1). The resonance of a bridge 2 methine proton, **Cys 14** (bridge 2 CH) that links the pyrrole ring at position 2 to the thioether bond of Cys 14 (Feng et al., 1990a), was found to have a 0.21 ppm chemical shift difference in Zn(II) Cyt *c* compared to Fe(II) protein.

Optical Absorption and Emission Spectroscopy. The protein environment would alter the optical spectrum of Zn porphyrin and give further information about ligation in Zn Cyt *c*. We modeled the protein with Zn porphyrins in different solvents and compared their spectra with that of Zn Cyt *c*.

The electronic absorption and emission spectra of Zn Cyt *c* are shown in Figure 6, along with the spectra of Zn(MP-DME) in two solvents; a noncoordinating solvent, toluene, and pyridine that offers a nitrogenous ligand. Absorption maxima of the visible region bands, relative extinction coefficients, and phosphorescence lifetimes of Zn Cyt *c*, Zn-(MP)-Mb, and Zn porphyrin model compounds are compiled in Table 2.

The absorption and emission spectra of the protein resemble the model compounds. However, the absorption spectrum of Zn Cyt *c* is red-shifted in comparison to the Zn(MP)-Mb and Zn(MP-DME) species. For instance, the Soret absorption maximum, is at 404, 414, 416, and 423 nm in Zn(MP-DME) in toluene, pyridine, Zn(MP)-Mb, and Zn Cyt *c*, respectively. The spectrum of Zn(MP) in pyridine (data not shown) does not differ from that of Zn(MP-DME), but Zn(MP) is not soluble in toluene. In the absorption spectrum of Zn Cyt *c* (Figure 6), the so-called "hyper" band is evident at 346 nm. A similar band was also present in the absorption spectrum of Zn(MP)-Mb at ~350 nm (Papp et al., 1990).

Finally, the phosphorescence lifetime of Zn Cyt *c* was compared with those of Zn porphyrin compounds. As seen in Table 2, the lifetime for Zn Cyt *c* was about one-third of that of model compounds.

DISCUSSION

Optical Spectroscopy. The absorption of unliganded Zn-(MP-DME) in toluene shows a strong α band and a weaker β band (Figure 6A). Ligation of neutral or anionic ligands to Zn porphyrin produces a red shift in the visible bands of the absorption spectrum and an increase of the extinction coefficient of the β band relative to that of the α band (Figure 6B) (Gouterman, 1959; Jansen & Noort, 1976; Vogel & Stahlbush, 1977; Nappa & Valentine, 1978). The absorption spectrum of Zn Cyt *c* is indicative of Zn having axial coordination, because it is red-shifted compared to model tetracoordinated Zn porphyrins and pentacoordinated Zn porphyrin compounds with a nitrogenous ligand (Figure 6C and Table 2). The absence of the metal−Met absorption band at 695 nm in Zn Cyt *c* is not necessarily related to the

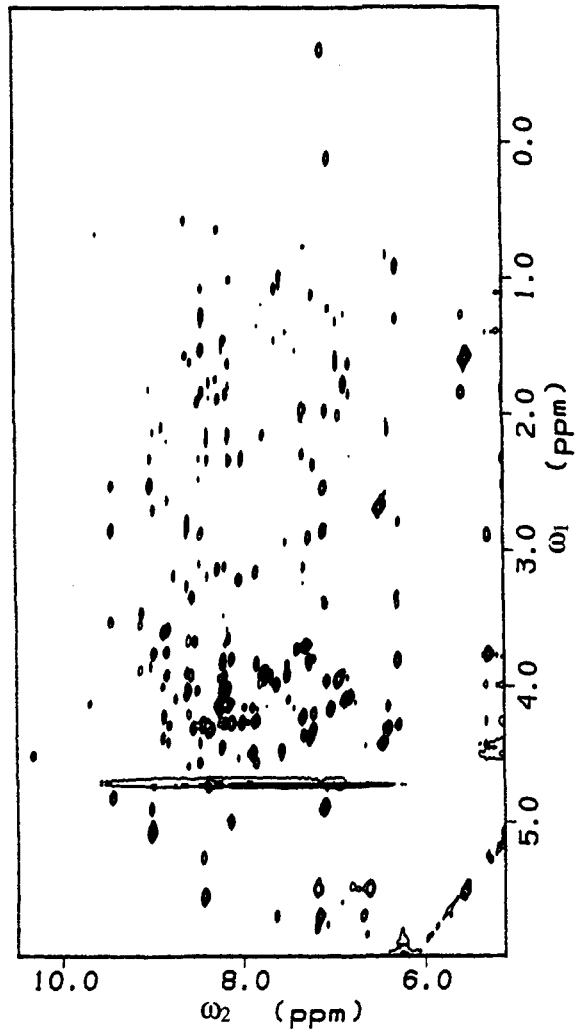

FIGURE 4: TOCSY-NMR spectrum of Zn Cyt *c* at 35 °C.

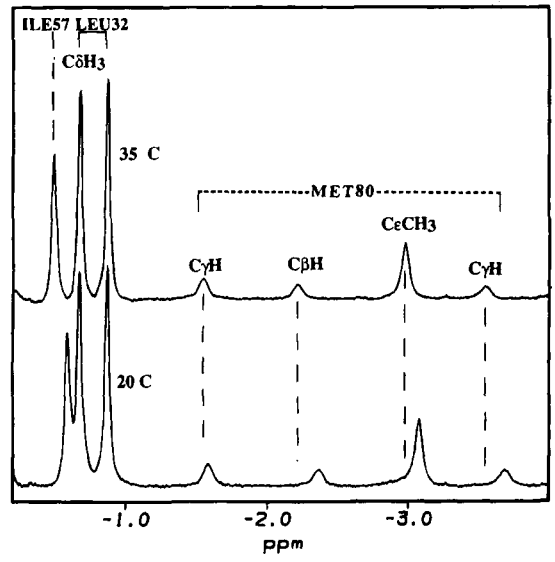

FIGURE 5: 1D-NMR spectra of Zn Cyt *c* in the upfield region at 20 and 35 °C.

lack of such a bond, which also is not detected in Fe(II) Cyt *c* (Schejter & Aviram, 1970) or cobalt Cyt *c* (Dickinson & Chien, 1975b). It seems that the 695-nm band manifests itself only in Fe(III) Cyt *c*, in spite of the fact that the Fe−S bond length is shorter in Fe(II) Cyt *c* (2.43 vs 2.35 Å for the yeast Fe(III) and Fe(II) protein, respectively).

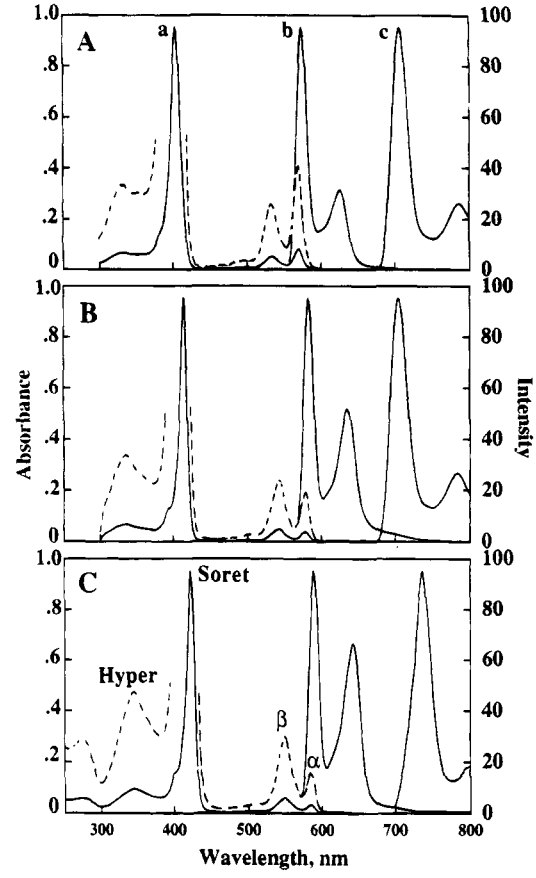

FIGURE 6: Optical spectra of Zn Cyt *c* and model Zn porphyrin compounds: (a) absorption, the scale of the enlarged spectrum is 0.2; (b) fluorescence emission; (c) phosphorescence emission using delay and gate times of 0.5 and 9 ms, respectively. The temperature for the absorption and fluorescence measurements was 20 °C and for phosphorescence was 77 K. Panels: (A) Zn(MP-DME) in toluene, fluorescence and phosphorescence λ_{exc} 404 nm; (B) Zn-(MP-DME) in pyridine, λ_{exc} 404 nm; (C) Zn Cyt *c* (~5 μM) in 10 mM phosphate buffer, pH 7.0, and 0.1 M NaCl, λ_{exc} 404 nm. The hyper, Soret, and α and β bands are labeled in the Zn Cyt *c* spectrum in panel C.

In terms of the hyper spectroscopic marker, the model Zn porphyrin compounds in coordinating solvents resemble Zn Cyt *c*. The absorption band at 354 nm (hyper band) has been considered as indicating sulfur ligation in Zn porphyrins (Nappa & Valentine, 1978). It is interesting that a hyper band is observed in the absorption spectrum of Zn(MP)-Mb (Table 2), where proximal His 93 is the axial ligand amino acid residue at a distance of 2.17 Å away from the metal center. Sulfur donors, like Met 55 or Met 131, are 16.15 and 16.72 Å away from the metal in deoxy Fe(II) Mb and are unlikely to coordinate to Zn (there are no Cys residues in Mb). Most probably His 93 remains the fifth axial ligand in Zn(MP)-Mb and causes the Soret band to split and blue shift (hyper band). For these reasons, the absorption spectrum of Zn Cyt *c*, although affirming an axially liganded Zn, does not necessarily prove what is the nature of ligand-(s). It seems that on the basis of the absorption spectra one cannot differentiate between an oxygen, sulfur, or nitrogen ligand.

The fluorescence and phosphorescence spectra of Zn Cyt *c* are similar to tetra- and pentacoordinated Zn porphyrin, although red-shifted (Figure 6). The phosphorescence lifetime of Zn Cyt *c* is significantly shorter than in the model system (Table 2) (Dixit et al., 1981, 1982). The presence

Table 2: Absorption Maxima at 298 K and Phosphorescence Emission Maxima and Lifetimes (τ) at 77 K of Model Zn Porphyrin Model Compounds and Proteins[a]

Zn porphyrins	absorption bands, nm				phosphorescence	
	Hyper	Soret	β	α	max, nm	τ, ms
Zn Cyt *c*	346 [16.6]	423 [157]	549 [10]	584 [5.1]	736	21[b]
Zn(MP)-Mb	354 [20.7]	416 [77]	544 [10]	583 [8.9]	700	71[c]
Zn(MP-DME)/toluene		404 [200]	532 [10]	569 [16.4]	707, 787	50[b,d]
Zn(MP-DME)/pyridine	335 [14.5]	414 [165]	543 [10]	578 [8.0]	705, 783	50[b]
Zn(MP-DME)-SBu[e]	354 [33.7]	438 [103]	562 [10]	596 [2.4]		*d*

[a] Numbers in brackets refer to the relative extinction, with the β band being normalized to 10. [b] This work; data taken from Figure 6. [c] Papp et al., 1990. [d] Nappa & Valentine, 1978. [e] SBu: *n*-butyl thiolate complex.

of the two sulfurs of covalently bound Cys 14 and Cys 17 may have an inductive effect, since they are less than 3 Å away from the closest pyrrole ring carbon on the porphyrin. As a result of such an effect, the spectrum will shift to higher wavelength and the phosphorescence lifetime will be lower. In addition, the electric field of the protein imposed on the porphyrin can be effective in shifting the spectra (Anni et al., 1994). The presence of the heavy sulfur atom in Met 80, directly over the porphyrin ring, may also serve to shorten the triplet lifetime.

Structure of Zn Cyt c. An early 1D-NMR spectroscopic study of Zn Cyt *c* has provided assignments of protons from 10 residues and the heme meso positions (Moore et al., 1980). In that work the spectra were not well resolved, and resolution did not improve at increasing temperatures, which was attributed to protein instability. We found that with our Zn Cyt *c* preparation there is no protein aggregation during the NMR measurements. The proton resonances of Zn Cyt *c* are well resolved, and most of them overlap within experimental error with those of Fe(II) Cyt *c* (Table 1, Figure 2). Residues could be assigned in every part of the protein, suggesting that no helix, β-turn, or loop had any major deviation from the native protein. Forty-eight residues are conserved in horse, yeast iso-1 and tuna Cyt *c*, and 30 of them (Table 1, residues in boldface) were identified in Zn Cyt *c*. These potentially important residues for structure and/or function were very similar, in terms of their proton resonances, in the two metal proteins. They include Phe 10, Phe 36, Phe 82, and Trp 59 with bulky side-chain aromatic rings, which are in the interior of the protein, as well as the hydrophobic residues Leu 68 and Leu 98. The positions of residues in the interface of Cyt *c* involved in the binding to its redox partners, like Cyt *c* peroxidase and Cyt *c* oxidase, are also conserved in Zn Cyt *c*. We located 9 out of the 14 residues (**Lys 8,** Ile 9, **Val 11**, Gln 12, **Lys 13**, **Cys 14**, **Ala 15**, **His 18**, **Thr 19**, Gly 29, **Asn 70**, **Tyr 74**, Ile 75, Ile 85) that are implicated in the Cyt *c*−C*c*P interface from the crystal structure of the complex (Pelletier & Kraut, 1992) and H−D exchange NMR measurements (Jeng et al., 1994). Finally, the structure of Zn Cyt *c* is temperature-dependent (Figure 5), as described also by Moore et al. (1980).

The most telling indication of the coordination of Zn comes from the identification of the resonances from the axial ligands, His 18 and Met 80. The chemical shifts for the backbone protons of His 18 and Met 80 are about the same in the two proteins. However, these protons are located quite far away from the metal (His 18 CαH−Fe, 6.77 Å; His 18 NH−Fe, 6.59 Å; Met 80 CαH−Fe, 5.38 Å; Met 80 NH−Fe, 6.66 Å). The backbone resonances therefore do not establish ligation of these residues. However, with a combination of 1D- and 2D-NMR (COSY, TOCSY, and NOESY) spectra, the proton resonances from side chains of His 18 and Met 80 were also identified. Their close identity with those of the Fe(II) protein means that the liganding residues are in the same position and suggest that both proteins possess hexacoordinated metal ions (Table 1). There are, though, small variations of 0.05 ppm in the chemical shifts of axial ligand proton resonances between Fe(II) Cyt *c* and the Zn derivative and some larger ones, up to 0.30 ppm. The latter may be ascribed to a change in the electron delocalization in the Zn porphyrin, and/or a change in the length of the Zn−ligand bond (probably the Zn−His 18 bond) and/or an altered bond angle between the porphyrin plane and the Zn−ligand bond.

Axial Ligands of Zn Cyt c. As commonly occurring ligands in Zn proteins are nitrogen from His residues, sulfur from Cys, and oxygen from H_2O, Glu, or Asp (Jernigan et al., 1994), the same axial ligands of Fe(II) and Fe(III) Cyt *c*, that is, His 18 and Met 80, could be employed by Zn Cyt *c*. There is no evidence that any amino acid, other than His 18 and Met 80, is an axial ligand to Zn Cyt *c*. Indeed, the chemical shifts of proton resonances from all residues, which could be considered as alternative ligands of Zn Cyt *c* (His 33, Lys 79, Phe 82), are not significantly different from those found in the native Fe protein. His 26 and/or His 33 (at neutral pH) and Lys 79 (at alkaline pH) have been found to compete with Met 80 for ligation to Fe, when major structural rearrangements occur in denatured Cyt *c* (Babul & Stellwagen, 1971; Muthukrishnan & Nall, 1991). His 82 takes the place of Met 80 in the Phe 82 → His 82 site-directed mutant of Fe Cyt *c* (Hawkins et al., 1994).

Zn Ligation in Model Compounds and Proteins. In proteins, Zn provides a nucleus of folding with four ligands in tetrahedral arrangement in 51 out of the 74 known crystal structures; there are also examples of tri- and pentacoordinated Zn proteins but none of a hexacoordinated protein (Jernigan et al., 1994). Since it seems that there are no naturally occurring Zn porphyrin proteins, to examine the possible ligation of Zn, we must turn to Zn porphyrin model compounds.

In model porphyrin compounds Zn is usually tetracoordinated in noncoordinating solvents (Gouterman, 1959; Jansen & Noort, 1976; Vogel & Stahlbush, 1977; Nappa & Valentine, 1978). Because Zn(II) with an atomic radius of ~1.25 Å is larger than Fe (radius: 1.17 Å), it was initially suggested that Zn would be out of plane (Collins & Hoard, 1970). Subsequently, it was shown by crystallography of tetracoordinated Zn porphyrins (Scheidt et al., 1978) and explained using a vibronic approach (Bersuker & Stavrov, 1988) that Zn is in-plane. This in-plane position of Zn was compensated by an expanded porphyrin core, compared to the corresponding tetracoordinated Fe porphyrin, the metal

to porphyrin pyrrole nitrogen distances being Zn−N 2.036 Å and Fe−N 1.972 Å (Scheidt et al., 1978, 1986). Because of the particularly tight intermolecular contacts in tetracoordinated Zn porphyrins, a pair of pyrrole rings tilts from the mean porphyrin core plane (Scheidt et al., 1986).

In the presence of N, S, O, or P donors Zn porphyrins are usually pentacoordinated (Gouterman, 1959; Jansen & Noort, 1976; Vogel & Stahlbush, 1977; Nappa & Valentine, 1978). Coordination of a fifth ligand to Zn has two important consequences on its geometry (Schauer et al., 1985; Scheidt et al., 1987; and references therein). First, Zn is displaced out of the porphyrin plane toward the ligand, and as a result the Zn−N (pyrrole) distance becomes longer than in tetracoordinated compounds. Second, there is a radial expansion of the porphyrin core size, in going from tetra- to pentacoordination, instead of expected contraction upon removal of bulky Zn from the center of the porphyrin.

A hexacoordinated geometry was initially precluded, because of the stereochemical constraints of the porphyrin core and the lack of any spectroscopic data supporting the existence "in solution" of a hexacoordinated Zn porphyrin. However, Zn porphyrins were crystallized with two axial ligands in an arrangement similar to that of hexacoordinated high-spin Fe(II) porphyrins (Schauer et al., 1985; Scheidt et al., 1987). In these cases Zn resides in-plane at the expense of an enlarged porphyrin core accomplished by means of a C_{2h} distortion. The Zn−N distances are shorter than in pentacoordinated Zn-porphyrins but still longer than tetracoordinated compounds. The axial ligands are weakly bound to Zn (Zn−O, 2.38 Å; Zn−N, 2.43 Å). The distances from Zn of other axial ligands like sulfur are expected to be different, with nitrogen being closer than sulfur (Hückel, 1951; Scheidt et al., 1986). In addition to distance correlations between Zn porphyrins and axial ligands, stereochemical hindrances, and electrostatic interactions, the hydrogen-bonding network and the interplay among these parameters would determine the axial ligands in each particular case.

In spite of the somewhat long distance between Zn and the axial ligands in porphyrin model compounds, the existence of a real axial interaction, albeit weak, is evident from the expansion of the porphyrin core. In a similar vein, the fluorescence line narrowing (FLN) studies of Zn Cyt *c* show that the vibrational line at 1603 cm^{-1} shifted to 1612 cm^{-1} when Zn Cyt *c* was denatured (Logovinsky et al., 1993). This line is considered as an indicator of the porphyrin "core size", and a shift to higher frequency would indicate a decrease in the core size. On the basis of model Zn porphyrins, the larger the core size becomes, the higher the ligation. Denatured native Fe protein is known to be hexacoordinated, but Zn in denatured protein would be most probably pentacoordinated as the protein constraint is relieved. A less rigid Zn conformation in denatured Cyt *c* is suggested by the width of the electronic transition, which is more than 5-fold larger than in the native state (Logovinsky et al., 1993). The data then would indicate that originally Zn in the protein had six ligands, and the trend in denaturation is higher frequency → smaller core size → fewer ligands. Finally, we compare the marker of the core size for the excited state in Zn Cyt *c* (1603 cm^{-1}) with that of the ground state in Fe(II) Cyt *c*, obtained by resonance Raman spectroscopy (1622 cm^{-1}) (Spiro & Strekas, 1972). A smaller frequency and bigger size for the porphyrin core are consistent with the larger size of the Zn metal. Absolute determination of the ligation state on the basis of fluorescence line narrowing would await the assignment of vibrational lines in model systems.

The presence of a hexacoordinated Zn porphyrin in a crystal may be due to a constrained environment and solid-state effects. Indeed, one axial ligand was disordered between two conformations, and coordination was lost on standing in the solid state (Schauer et al., 1985). Therefore, on the basis of the model porphyrins, it would seem unlikely that Zn is hexacoordinated in Cyt *c*, yet we have to entertain the possibility that the protein matrix may also constrain the atoms, so that hexacoordination is favored. Furthermore, the coordination geometry of Zn exhibited in crystals of small molecules does not necessarily apply to proteins. In an extended absorption fine structure (EXAFS) study of small Zn peptides (18mers), designed to mimic the local Zn environment in Zn-finger proteins (His_2-Zn-Cys_2, His_1-Zn-Cys_3, Cys_2-Zn-Cys_2), it was found that the Zn−ligand distances are consistently longer in the peptide than in the protein (Chance et al., 1992). This suggests that the protein compresses somewhat the metal−ligand sites.

Other metals in Cyt *c* derivatives like cobalt (Co) (Dickinson & Chien, 1975a,b), nickel (Ni) (Findlay & Chien, 1977), and copper (Cu) (Findlay et al., 1977) are reported to be in a hexacoordinated state. However, Findlay and Chien (1977) showed that the Ni−Met 80 bond is weaker than in the native protein because of the antibonding electrons in Ni Cyt *c*. The same also holds true in the case of Co Cyt *c*. The coordination state of Cu in Cyt *c* was debated recently, and it was proposed on the basis of Raman spectroscopy and molecular orbital calculations that it is a pentacoordinated species (Shelnutt et al., 1984) and that the observed shifts in the protein derive from addition of a σ-donating axial ligand. In contrast, manganese (Mn) in Cyt *c* (Dickinson & Chien, 1977) is pentacoordinated, with the metal displaced out of plane toward the side of His 18 (ionic radius 0.82 Å).

Our data demonstrate that introduction of Zn in Cyt *c* does not perturb the overall structure of the protein. Instead, Zn like iron serves as a stabilizing nucleus for the cytochrome. Although Zn dictates pentacoordination in model porphyrin compounds, the protein imposes hexacoordination in Zn Cyt *c* with both His 18 and Met 80 axial ligands conserved and without any disordering at least of the local peptide chain(s). Consequently Zn porphyrin in the cytochrome is in an extraordinary hexacoordinated state, and the protein conformation is the same for the two divalent metals, Fe(II) and Zn(II).

ACKNOWLEDGMENT

We thank Dr. G. Brayer for providing the coordinates of horse Fe(III) Cyt *c*. We also thank Drs. Walter Englander and Paul Angiolillo for stimulating conversations and use of equipment.

REFERENCES

Anni, H., Vanderkooi, J. M., Sharp, K. A., Yonetani, T., Hopkins, S. C., Herenyi, L., & Fidy, J. (1994) *Biochemistry 33*, 3475−3486.

Babul, J., & Stellwagen, E. (1971) *Biopolymers 10*, 2359−2361.

Babul, J., & Stellwagen, E. (1972) *Biochemistry 11*, 1195−2000.

Bax, A., & Davis, D. G. (1985) *J. Magn. Reson. 65*, 521−528.

Berghuis, A. M., & Brayer, G. D. (1992) *J. Mol. Biol. 223*, 959−976.
Bersuker, I. B., & Stavrov, S. S. (1988) *Coord. Chem. Rev. 88*, 1−68.
Bushnell, G. W., Louie, G. V., & Brayer, G. D. (1990) *J. Mol. Biol. 214*, 585−595.
Chance, M. R., Sagi, I., Wirt, M. D., Frisbie, S. M., Scheuring, E., Chen, E., Bess, J., Henderson, L. E., Arthur, L. O., South, T. L., Perez-Alvarado, G., & Summers, M. F. (1992) *Proc. Natl. Acad. Sci. U.S.A. 89*, 10041−10045.
Collins, D. M., & Hoard, J. L. (1970) *J. Am. Chem. Soc. 92*, 3761−3771.
Dickinson, L. C., & Chien, J. C. W. (1975a) *Biochemistry 14*, 3526−3534.
Dickinson, L. C., & Chien, J. C. W. (1975b) *Biochemistry 14*, 3534−3542.
Dickinson, L. C., & Chien, J. C. W. (1977) *J. Biol. Chem. 252*, 6156−6162.
Dixit, B. B. S. N., Waring, A., Wells, K., Wong, P., Woodrow, G. V., & Vanderkooi, J. M. (1982) *Eur. J. Biochem. 126*, 1−9.
Dixit, S. N., Waring, A. J., & Vanderkooi, J. M. (1981) *FEBS Lett. 125*, 86−88.
Feng, Y., Roder, H., & Englander, S. W. (1990a) *Biophys. J. 57*, 15−22.
Feng, Y., Roder, H., & Englander, S. W. (1990b) *Biochemistry 29*, 3494−3504.
Findlay, M. C., & Chien, J. C. W. (1977) *Eur. J. Biochem. 76*, 79−83.
Findlay, M. C., Dickinson, L. C., & Chien, J. C. W. (1977) *J. Am. Chem. Soc. 99*, 5168−5173.
Fisher, W. R., Taniuchi, H., & Anfinsen, C. B. (1973) *J. Biol. Chem. 248*, 3188−3195.
Gouterman, M. (1959) *J. Chem. Phys. 30*, 1139−1161.
Green, T. J., Wilson, D. F., Vanderkooi, J. M., & DeFeo, S. P. (1988) *Anal. Biochem. 174*, 73−79.
Hamada, D., Hoshio, M., Kataoka, M., Fink, A. L., & Goto, Y. (1993) *Biochemistry 32*, 10351−10358.
Hawkins, B. K., Hilgen-Willis, S., Pielak, G. J., & Dawson, J. H. (1994) *J. Am. Chem. Soc. 116*, 3111−3112.
Ho, P. S., Sutoris, C., Liang, N., Margoliash, E., & Hoffman, B. M. (1985) *J. Am. Chem. Soc. 107*, 1070−1071.
Hückel, W. (1951) *Structural Chemistry of Inorganic Compounds*, Vol. 2, 588 pp, Elsevier, New York.
Jansen, G., & Noort, M. (1976) *Spectrochim. Acta 32A*, 747−753.
Jeng, M.-F., Englander, S. W., Pardue, K., Rogalskyj, J. S., & McLendon, G. (1994) *Nature Struct. Biol. 1*, 234−238.
Jernigan, R., Raghunathan, G., & Bahar, I. (1994) *Curr. Opin. Struct. Biol. 4*, 256−263.
Koloczek, H., Horie, T., Yonetani, T., Anni, H., Maniara, G., & Vanderkooi, J. M. (1987) *Biochemistry 26*, 3142−3148.
Kraulis, P. J. (1991) *J. Appl. Crystallogr. 24*, 946−950.
Liang, N., Kang, C. H., Ho, P. S., Margoliash, E., & Hoffman, B. M. (1986) *J. Am. Chem. Soc. 108*, 4665−4666.
Liang, N., Pielak, G. J., Mauk, A. G., Smith, M., & Hoffman, B. M. (1987) *Proc. Natl. Acad. Sci. U.S.A. 84*, 1249−1252.
Logovinsky, V., Kaposi, A. D., & Vanderkooi, J. M. (1993) *Biochim. Biophys. Acta 1161*, 149−160.
Louie, G. V., & Brayer, G. D. (1989) *J. Mol. Biol. 210*, 313−322.
Louie, G. V., & Brayer, G. D. (1990) *J. Mol. Biol. 214*, 527−555.
Louie, G. V., Pielak, G. J., Smith, M., & Brayer, G. D. (1988) *Biochemistry 27*, 7870−7876.
Macura, S., & Ernst, R. R. (1980) *Mol. Phys. 41*, 95−117.
Marion, D., & Wüthrich, K. (1983) *Biochem. Biophys. Res. Commun. 113*, 967−974.
Moore, G. R., Williams, R. J. P., Chien, J. C. W., & Dickinson, L. C. (1980) *J. Inorg. Chem. 12*, 1−15.
Muthukrishnan, K., & Nall, B. T. (1991) *Biochemistry 30*, 4706−4710.
Nagayama, K., Kumar, A., Wüthrich, K., & Ernst, R. R. (1980) *J. Magn. Reson. 40*, 321−334.
Nappa, M., & Valentine, J. S. (1978) *J. Am. Chem. Soc. 100*, 5075−5080.
Papp, S., Vanderkooi, J. M., Owen, C. S., Holtom, G. R., & Phillips, C. M. (1990) *Biophys. J. 58*, 177−186.
Pelletier, H., & Kraut, J. (1992) *Science 258*, 1748−1755.
Qi, P. X., Di Stefano, D. L., & Wand, A. J. (1994) *Biochemistry 33*, 6408−6417.
Redfield, A. G., & Kuntz, S. D. (1975) *J. Magn. Reson. 19*, 250−254.
Schauer, C. K., Anderson, O. P., Eaton, S. S., & Eaton, G. R. (1985) *Inorg. Chem. 24*, 4082−4086.
Scheidt, W. R., Kastner, M. E., & Hatano, K. (1978) *Inorg. Chem. 17*, 706−710.
Scheidt, W. R., Mondal, J. U., Eigenbrot, C. W., Adler, A., Radonovich, L. J., & Hoard, J. L. (1986) *Inorg. Chem. 25*, 795−799.
Scheidt, W. R., Eigenbrot, C. W., Ogiso, M., & Hatano, K. (1987) *Bull. Chem. Soc. Jpn. 60*, 3259−3533.
Schejter, A., & Aviram, I. (1970) *J. Biol. Chem. 245*, 1552−1557.
Shelnutt, J. A., Straub, K. D., Rentzepis, P. M., Gouterman, M., & Davidson, E. R. (1984) *Biochemistry 23*, 3946−3954.
Spiro, T. G., & Strekas, T. C. (1972) *Proc. Natl. Acad. Sci. U.S.A. 69*, 2622−2626.
Stellwagen, E., Rysavy, R., & Babul, G. (1972) *J. Biol. Chem. 247*, 8074−8077.
Takano, T. (1977) *J. Mol. Biol. 110*, 569−584.
Vanderkooi, J. M., & Erecinska, M. (1975) *Eur. J. Biochem. 60*, 199−207.
Vanderkooi, J. M., & Landesberg, R. (1977) *FEBS Lett. 73*, 254−256.
Vanderkooi, J. M., Adar, F., & Erecinska, M. (1976) *Eur. J. Biochem. 64*, 381−387.
Vanderkooi, J. M., Landesberg, R., Haydon, G., & Owen, C. (1977) *Eur. J. Biochem. 81*, 339−347.
Vanderkooi, J. M., Glatz, P., Casadei, J., & Woodrow, G. V., III (1980) *Eur. J. Biochem. 110*, 189−196.
Vogel, G. C., & Stahlbush, J. R. (1977) *Inorg. Chem. 16*, 950−953.
Wand, A. J., Di Stefano, D. L., Feng, Y. Q., Roder, H., & Englander, S. W. (1989) *Biochemistry 28*, 186−194.
Wüthrich, K. (1986) *NMR of Proteins and Nucleic Acids*, pp 13−34, J. Wiley & Sons, New York.
Zhou, J. S., & Hoffman, B. M. (1994) *Science 265*, 1693−1696.

BI9424205